A Microchip for Continuous-Flow, Magnetically Controlled Capture and Separation of Microparticles

Yao Zhou[1], Yi Wang[2], and Qiao Lin[1*]

[1]Department of Mechanical Engineering, Columbia University, New York 10027, U.S.A.
[2]CFD Research Corporation, Huntsville, Alabama 35805, U.S.A.

Abstract

This paper presents a novel microfluidic chip that exploits magnetic manipulation for integrated capture and separation of microparticles in continuous flow. The chip integrates an active-mixing enhanced incubator and a magnetic fractionation-based separator. In the incubator, surface-functionalized magnetic beads are used to capture target particles by specific binding, which is promoted by active mixing effected by judiciously applied magnetic forces. Subsequently in the separator, the captured target particles are then separated, and thereby retrieved, in the same magnetic field. In contrast to currently existing devices that are limited by manual off-chip incubation, slow batch-mode operation, or complicated fabrication processes, our device offers automated and continuous operation with a simple structure design. The incubator and separator, as well as the chip that integrates these components, are fabricated using soft lithography techniques and systematically characterized under varying operating conditions including target to non-target particle ratios, 1:1 and 1:10. With experimentally demonstrated reliability, flexibility and separation efficiency (>90%), the device holds great promise for sorting, purification, enrichment, and detection of cells in lab-on-chip systems.

1. Introduction

Microfluidic particle separation involves the isolation and collection of target particles from impure samples, and is widely used in sorting, purification, enrichment and detection of cells [1-4] in cell biology, drug discovery, and clinical diagnostics. A number of methods currently exist for particle separation on microfluidic platforms, such as size-based separation [5-9], acoustic separation [10], dielectrophoresis [11, 12], fluorescence-activated [13, 14] and magnetic-activated separation [15, 16]. Among these, methods based on magnetic control are particularly attractive, which utilize surface-functionalized magnetic beads to capture target particles through specific binding, and then separate the target particles by magnetic manipulation. This separation scheme relies on the interaction of chemical bonds rather than geometrical or physical properties of the particles, and hence allows highly specific and selective particle separation.

* Corresponding author

Email: qlin@columbia.edu

Phone: +01-212-854-1906

There are two operating modes for magnetically based microfluidic particle separation: batch mode and continuous-flow mode. The batch mode typically involves retention of target-bound magnetic beads on the channel floor by magnetic force and subsequent release after the non-target particles are rinsed out. For instance, magnetic bead beds [17] and sifts [18] are developed to capture target particles; however, these methods only offer limited separation efficiency. To enhance separation efficiency, a number of batch-mode magnetic separation chips have been developed employing magnet designs involving a quadruple electromagnet [19], a planar electromagnet [20], or nickel posts [21]. Further, the planar electromagnet can be incorporated on chip with microvalves and micropumps to form fully automated functionalities such as fluid actuation and particle mixing [15]. However, batch-mode designs suffer from several inherent limitations including prolonged durations of operation, complicated fluidic handling, and most importantly, significant contaminanation due to non-specific trapping of impurities that are sequestered in the bead mass [22].

In contrast, continuous-flow magnetic particle separation, which employs the continuous accumulative spatial deflection of magnetic beads (also termed fractionation), effectively mitigates the aforementioned limitations. This method can be further classified into two categories according to whether an integrated magnet or off-chip magnet is used. In the first category, magnetic microstrips, of typically alloy or ferromagnetic materials, are deposited on the device substrate to generate a magnetic field gradient that separates magnetic beads [23, 24]. Substantial effort is required to design and fabricate on-chip magnetic strips as well as fluidic components to ensure balanced hydrodynamic and magnetic forces. Alternatively in the second category, the use of a simple external magnetic setup in conjunction with on-chip separation enables salient flexibility in device design and magnetic manipulation [16, 25]. Despite these notable features, existing magnetic separators typically share a common issue in that prolonged off-chip incubation of target cells with magnetic beads is required to ensure their sufficient binding before on-chip separation. This is time-consuming, labor-intensive, and prone to contamination during sample transfer, and could potentially cause the damage or loss of viability to the target cells. Seamless integration of an on-chip incubation module, in which target cells are captured by magnetic beads prior to separation, would effectively address this issue and is hence highly desired.

A suitable on-chip mixing technique is key to the on-chip incubation module. Due to low-Reynolds flow and molecular diffusion-dominated transport mechanism inside the micron-sized channels, a variety of passive and active approaches are investigated to enhance mixing in the incubation process [26-28]. Passive micromixers entirely rely on diffusion or chaotic advection [29, 30] without external energy, and hence, are inadequate for particle/bead mixing and prone to undesired bead retention/trapping at the corners and channels. On the other hand, existing active mixers utilize flow agitation arising from an external field (e.g., acoustic [31] or electro-hydrodynamic [32, 33]) to enhance mixing, and typically require additional fabrication and operation efforts.

In this paper, we present a novel integrated microfluidic chip for continuous-flow magnetically actuated capture and separation of target particles. As a major significant feature, the device incorporates the on-chip integration of an active mixing-enhanced incubator with a magnetic fractionation-based separator to achieved fully automated sample processing of particles or cells. The incubator features a serpentine-shaped

channel design, which in the presence of a properly configured magnetic field enables effective mixing and capture of target particles by surface-functionalized magnetic beads. The separator, with zero dead volume, is located at the downstream of the incubator and exploits the magnetic force to selectively direct the target particle-bead complex into a lateral buffer stream to achieve fractionation. The chip is fabricated with soft lithography methods and systematically characterized. Experimental results demonstrated that the device offers excellent processing throughput, separation efficiency (>90%), and operating flexibility.

The paper is organized as follows. The principle and design of the microchip is introduced in Section 2, which is followed by a description of the microchip fabrication and experimental setup in Section **Error! Reference source not found.**. Individual modules of the incubator and the separator are characterized in Section 4, first by examining the particle distribution across the channel width at different locations, and then by a thorough investigation of the integrated device in terms of fully automated functionality and separation efficiency. Finally, concluding remarks are given in Section 5.

2. Principle and Design

In this section, we will first elucidate the principle of the magnetically controlled capture and separation. Then, we will describe the device design and operating procedure.

The sample presented to our microchip contains a mixture of target microparticles, whose surfaces are functionalized with a biomolecule (or a ligand), and non-target particles. These particles are a model of target and non-target cells in a biological sample. Magnetic microbeads, whose surfaces are immobilized with a receptor molecule that specifically recognizes the ligand on the target particles, are introduced into the sample. Binding between the receptor and ligand leads to the formation of complexes of target particles and magnetic beads. As a result, the target particles are captured by the magnetic beads. This capture process is facilitated by a prudently applied magnetic field, under which the magnetic beads will traverse the sample, achieving mixing with particles in the sample. The captured target particles are subsequently separated from non-target particles by isolating the particle-bead complexes using the same magnetic field. For purposes of proof of concept, we use biotin as a ligand on the target particles, while streptavidin is used as a receptor on the magnetic beads. As such, our method can be readily extended to manipulation of biological samples. For example, target cells can be captured and isolated using magnetic beads functionalized with receptor molecules specifically recognizing membrane proteins on the cells.

This particle capture and isolation concept is realized with a microchip consisting of two operating stages. First, in the incubation stage, magnetic beads are mixed in the sample and capture target particles via specific ligand-receptor binding. Next, in the separation stage, complexes of target particles and magnetic beads resulting from the incubation step are separated from non-target particles for further analysis. In the microchip design (Figure 1), an incubator and a separator are connected in series, and are placed next to a bar-shaped permanent magnet. In the incubator, two inlets, respectively termed “sample inlet” and “bead inlet”, are used to introduce the particle sample and magnetic beads, respectively. The inlets are merged at a Y-junction and followed by a

serpentine microchannel (termed "incubation channel"), which consists of a series of parallel channels connected by U-shaped turns that allow mixing of magnetic beads and capture of target particles.

During operation, low Reynolds number conditions allow the fluids introduced into the device via the sample and bead inlets to flow side by side as two laminar streams throughout the incubator. In the absence of a magnetic field, target and non-target particles as well as magnetic beads would also remain in the respective fluid streams, with lateral diffusive mixing negligible due to their relatively large sizes. Now, under the permanent magnet's magnetic field, which is directed laterally with respect to the straight incubation channels, acts to pull the magnetic beads toward the magnet (i.e., to the left in Figure 1a). Thus, the magnetic beads, which initially are located in the right-side stream in the leftmost straight section of the incubator channel, are pulled towards the channel's left side and cross the flow streamlines. Immediately after passing the first U-turn, the magnetic beads follow the streamlines and emerge again on the right side when entering the next straight incubator channel section. As they move downstream, however, the magnetic beads are pulled back to the channel's left side. Such lateral movement of magnetic beads is repeated in all of the subsequent straight sections of the incubator channel. Thus, as shown in their trajectory of the magnetic beads before and after the 1st turn in Figure 1a, magnetic beads will transversely cross the stream in each straight channel section. Due to the alternating configurations of the serpentine channel, the accumulative effect of repeated stream crossing allows sufficient interaction of magnetic beads with target particles, allowing the target particles to be captured by the beads. The magnetic pulling force experienced by the beads may vary along the incubation channel depending on their distance from the magnet. Therefore, an incubator with consistent performance requires that the ratio of the magnetic force to the hydrodynamic force remain mostly constant throughout the channel sections. This will effectively eliminate issues of particle retention in the upstream channel sections (which are relatively close to the magnet) and inadequate bead deflection in the downstream sections (which are relatively far away from the magnet). Therefore, our incubator design employs a gradual increase in the channel section width proportional to their distance from the magnet (Figure 2), in which flow retardation allows for longer residence times in the downstream channel sections to compensate for the weakened magnetic force.

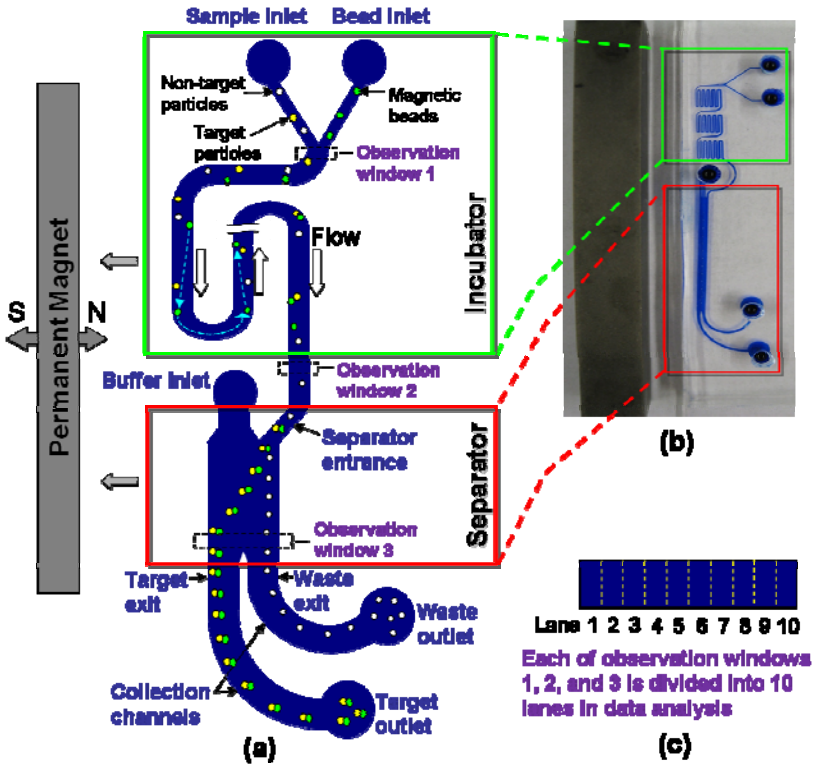

Figure 1. Microfluidic chip for continuous-flow, magnetically controlled capture and separation of microparticles. (a) Schematic of configuration and principle of the chip. It consists of a serially connected incubator and separator placed next to a bar-shaped permanent magnet. (b) A fabricated chip (with ink solution filled in the channels for enhanced clarity). (c) Lane division and designation at the three observation windows: Y-junction, the end of the incubator, and the end of the separator.

The bead-captured target particles emerge from the incubator and enter the separator, where they are fractionated from the non-target particles. The separator includes an additional inlet ("buffer inlet"), which merges with the separator entrance into a wide straight channel. A buffer stream free of particles and beads is introduced into the buffer inlet, which merges with the mixture of bead-captured target particles and non-target particles that has just exited the incubator. The mixture may also include a small number of uncaptured target particles or unused magnetic beads; they do not interfere with the separation process and hence will be ignored in the following discussion. The buffer and mixture will form two side-by-side laminar streams in the separator channel. As they move downstream in the separator channel, the bead-bound target particles are attracted towards the magnet, crossing the buffer stream and becoming separated from the non-target particles that remain in the sample stream. Thus, two outlets at the end of the collection channels following the separator channel, termed "target outlet" and "waste outlet", can be used to collect the bead-captured target particles and non-target particles, respectively. As the flow rate of the sample at the separator entrance is considerably less than that of the buffer at the buffer inlet, the non-target particles that remain in the sample stream will be constrained within a very thin layer near the right side wall of the separator channel, which will then completely exit through the waste exit. Therefore the bead-captured targets collected at the target outlet will be purified (i.e., free of non-target particles). This effectively addresses the limited degree of purification in most batch-

mode magnetic separation processes due to the false trapping of non-target particles. Also, the flow rates for the buffer and mixture streams are judiciously selected to produce adequate hydrodynamic force and prevent magnetic beads from sticking at the channel walls.

3. Experimental

The device consists of a sheet of poly(dimethylsiloxane) (PDMS) bonded to a glass slide (Figure 1b). The channel features were fabricated in the PDMS sheet using soft lithography techniques. Briefly, the fabrication process began with spin-coating and patterning of a 30-μm layer of SU-8 2025 photoresist (MicroChem, MA) on a silicon wafer, which upon curing at 95 ^{o}C for 5 min on a hotplate formed a master defining the negative of desired microfluidic features. Next, a PDMS prepolymer (Sylgard 184, Dow Corning, MI) was cast against the master and cured at 70 ^{o}C for 35 min, also on the hotplate. The resulting PDMS sheet was then peeled off from the master, cut into properly sized pieces, and punched with inlet and outlet holes. The PDMS was bonded to a glass slide after 10 min-treatment in a UV ozone cleaner (Model T10X10/OES, UVOCS, PA). Tygon tubes were inserted into the inlet and outlet holes in the PDMS and affixed with Epoxy to establish fluidic interconnects. Figure 1b illustrates the integrated chip with ink solution filled in the channels.

Materials including 5% bovine serum albumin (BSA) (Sigma-Aldrich, MO), 2.8 μm streptavidin-coated magnetic beads, 0.4 μm biotin-coated green fluorescent polystyrene particles (as target particles), and 0.4 μm uncoated red fluorescent polystyrene particles (as non-target particle) (all from Spherotech, IL) were used in the experiments. Three samples were prepared for different experiments: a) a suspension of streptavidin-coated magnetic beads (0.5% w/v) supplemented with BSA; b) a suspension of biotin-coated particles (0.1% w/v), and uncoated particles (0.1% w/v), supplemented with BSA (target vs. non-target ratio is 1:1); and c) a suspension of biotin-coated particles (0.05% w/v), and uncoated particles (0.5% w/v), supplemented with BSA (target vs. non-target ratio is 1:10). DI water was used as running buffer supplied to the separator. Before the experiments, the microfluidic channels were incubated with 2% BSA solution for 2 hours to block nonspecific binding, and then flushed with DI water. Samples and buffer were driven into respective inlets of the chip using syringe pumps (KD210P, KD Scientific, MA and NE-1000, New Era Pump System, NY). A 50 mm long bar-shaped Neodymium permanent magnet (McMaster-Carr, IL) was placed alongside the chip. Bright field and fluorescent images were taken on an inverted epi-fluorescent microscope (Diaphot 300, Nikon Instruments, NY) and recorded by a CCD camera (Model 190CU, Micrometrics, NH). Images were analyzed and quantitative data were extracted using ImageJ (available free online at http://rsb.info.nih.gov/ij/).

4. Results and Discussion

In this section, we will first characterize the incubator and separator separately by examining and comparing particle distributions across the channel widths at their exits. Then the performance of integrated device will be analyzed at multiple locations to demonstrate its capability of capture and separation of target particles.

4.1 Incubator

First, we examined the efficiency of active mixing in the incubator. With the permanent magnet bar placed to the immediate left of the chip (Figure 1), we injected magnetic beads from the bead inlet, and a suspension of target and non-target particles from the sample inlet.

Figure 2 is a snapshot image of the trajectories of magnetic beads within the incubator. It clearly shows that after passing each turn the magnetic beads traverse the flow stream and move towards the left side of each straight channel section, which markedly improves the contact probability and mixing between the beads and the particles. Although a moderate number of magnetic beads could be retained at the turns during operation, the bead inflow and outflow at the turns will eventually reach equilibrium, thus the number of beads retained will not increase infinitely and cause channel clogging. Also, the retained beads can be easily flushed through by judiciously increasing the flow rate and/or reducing the magnetic force at the end of the operation (results not shown), which will avoid bead loss.

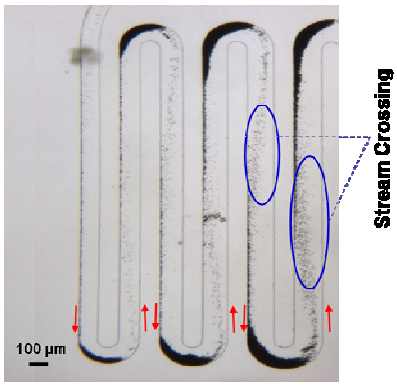

Figure 2. Image of active mixing by stream crossing of magnetic beads in the incubator.

Next, we quantitatively examined the incubator performance in terms of particle capture at the Y-junction of incubator inlets and the incubator exit, and compared the differential effects of the magnetic force on the target and non-target particles. To quantify the distribution of the bead-captured target particles and non-target particles across the channel, we divided the detection window into 10 lanes of equal widths along the channel width (Figure 1c) and calculated the percentage of target or non-target particles that fall within each lane by integrating the measured fluorescent intensity along the lane width. Figure 3 (a and b) illustrates the fluorescent images of target (green) and non-target (red) particles at the Y-junction of the incubator. The particles and magnetic beads suspension form two distinctive, side-by-side streams (respectively in the upper and lower halves of the Y-junction) with negligible mixing. Figure 3c quantitatively depicts the distributions of target and non-target particles at the Y-junction. It can be seen that the target and non-target particles are both highly concentrated in Lanes 1–5, which combine to contain 95.4% and 91.0% of the target and the non-target particles. This indicates that the particles have not yet mixed with the magnetic beads, which are contained in Lanes 6-10 where there is only a small percentage of target and non-target particles.

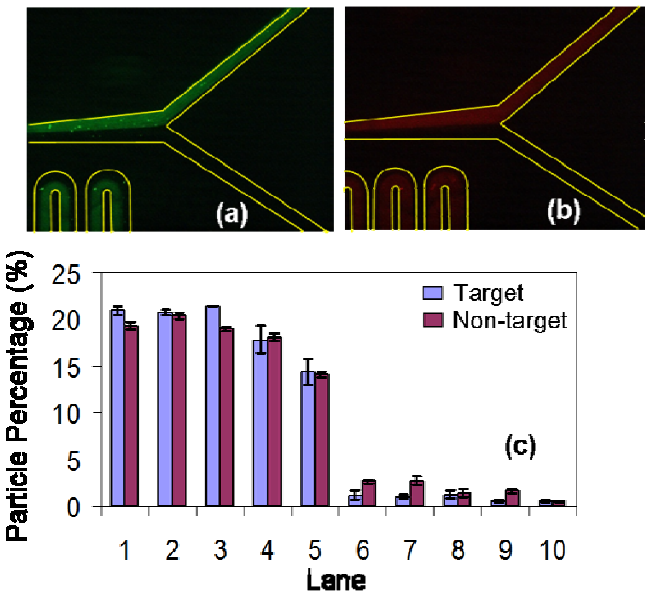

Figure 3. Distribution of target and non-target particles across the channel width at the Y-junction. Fluorescent micrograph of (a) target particles and (b) non-target particles at the Y-junction. (c) Percentage distribution of target and non-target particles across channel width at the Y-junction.

Next, we investigated the particle distributions at the end of the incubator. The fluorescent images of target (green) and non-target (red) at the end of the incubator are given in Figure 4 (a and b). It can be seen that the target particles captured by the magnetic beads in the serpentine channel are mostly attracted to the left, where the permanent magnet is placed. On the other hand, the free non-target particles spread out and distribute uniformly across the channel width due to their diffusion and flow agitation in the serpentine channel.

The quantitative particle distributions across the channel width at the end of the incubator are extracted and plotted in Figure 4c. Most target particles (95.9%) appear on the left half of the channel, whereas the non-target particles are evenly distributed across the channel width. The highest concentration of target particles does not occur in Lane 1, which may be attributed to the slight magnetization of target-bound magnetic beads and their aggregation on the left channel wall. Upon magnetization, the target-bound magnetic beads tend to aggregate into an oval-shaped cloud with the size of tens of microns, which is a few times larger than the lane width (20 μm). Therefore, when the oval cloud is attracted to the left side of the channel, Lane 1 only samples the edge of the oval containing a small number of target particles, whereas the center of the oval containing more target particles falls in Lane 2. The aggregation of magnetic beads also causes local discontinuity in bead flow as observed.

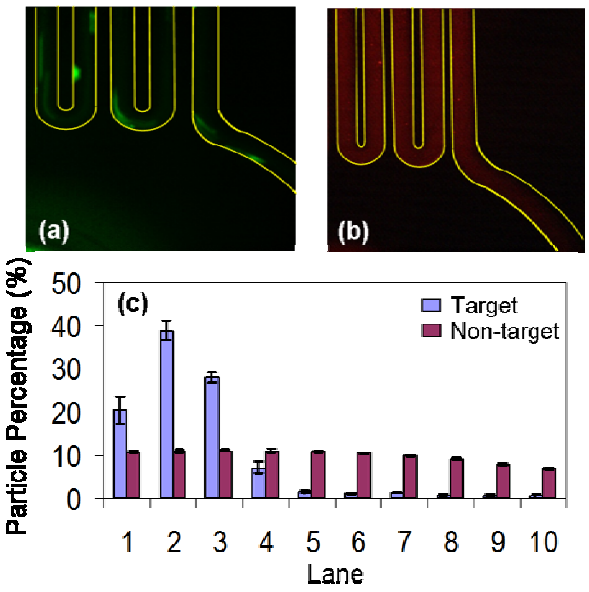

Figure 4. Distribution of target and non-target particles across channel width at the end of the incubator. Magnet is placed to the left of the incubator channel. Fluorescent micrograph of (a) target particles and (b) non-target particles at the end of the incubator. (c) Percentage distribution of target and non-target particles across channel width at the end of the incubator.

4.2 Separator

Next, we characterized the separator in terms of its capacity to deflect and extract magnetic beads. For this study, we fabricated a chip that only contains the separator. The permanent magnet was again placed to the left of the chip. A suspension of bare magnetic beads was introduced into separator entrance at a flow rate of 1 μL/min, while DI water was introduced into the buffer inlet at 4 μL/min. As shown in Figure 5a, when first entering the separation channel from the separator entrance, the beads are highly concentrated to the right side of the separator due to laminar flow behavior. As they migrate through the channel, they are attracted towards the magnet and accumulate at the left-hand side when exiting the separator (Figure 5b). For experimental control, the same procedures were carried out in the absence of the magnet, and results are compared.

Bead distributions across the channel width at the separator exit in the cases with and without the magnet are compared. An observation window at the separator exit was selected, where the channel width was again divided into 10 lanes and the percentage of beads falling into each lane was obtained to quantify the bead distributions. As the target and waste collection channels (Figure 1a) have similar hydrodynamic resistances, beads (and particles) located in the left five lanes will exit via the target exit, while those in the right five lanes will exit from the waste exit. As shown in Figure 5c, the magnetic force causes the beads concentrate to the left, with 90.3% located Lane 1, and 96.2% fall within Lanes 1-5. On the other hand, without the magnetic field, the majority of beads remain in the right lanes, with 96.7% of them in Lanes 6-10 and exiting from the right exit (Figure 5c). These results substantiate that the deflection and separation of the magnetic beads from its original streams is indeed caused by the presence of the magnetic field.

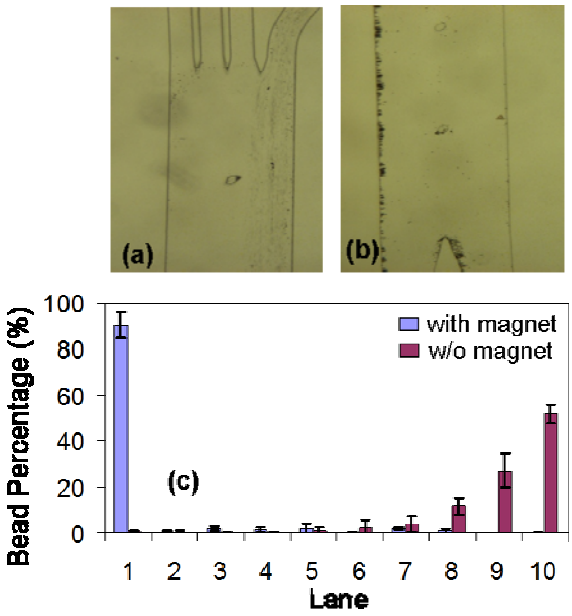

Figure 5. Characterization of fractionation capacity at the separator using bare magnetic beads. (a) Image at the separator inlet. Magnetic beads enter the separator from the right. (b) Image at the separator exit. (c) Percentage distribution of magnetic beads at the separator exit.

4.3 Integrated Microchip

Having characterized the individual modules, we then investigate a complete device that integrates an incubator and separator. With the same experimental setup, we inject a suspension of premixed target and non-target particles into the device's incubator via the sample inlet, and a suspension of magnetic beads via the bead inlet, each at a flow rate of 0.5 µL/min. The particle suspension sample is prepared at two count ratios (1:1 and 1:10) of target particle to non-target particle. DI water is infused via the buffer inlet into the device's separator at a flow rate of 4 µL/min. We examine particle distributions at the end of the separator to examine the ability of the integrated device to capture, isolate and extract target particles.

Figure 6 (a and b) presents fluorescence images of target and non-target particles, from a sample of 1:1 target to non-target ratio, taken within the separator observation window (Figure 1a) immediately upstream of the separator exits. It can be seen that the target and non-target particles are clearly separated at the left and right side of the channel with negligible overlap. Distributions of the particles are extracted from the experimental data and plotted in Figure 6c**.** The majority of the target particles (bound with magnetic beads) are attracted to the left side of the channel, with 87.0% of them contained in Lane 1, while the non-target particles remain in Lanes 9 and 10. Overall, 92.7% of target particles were retrieved at the target outlet (corresponding to Lanes 1-5), while 99.9% of the non-target particles were collected at the waste outlet.

Results obtained from a particle suspension sample with 1:10 mixing ratio are qualitatively the same (Figure 7), except that lower fluorescent intensities are measured due to the lower relative concentration of target particles in the sample. Specifically, 88.0% of the target particles are obtained in Lane 1. Overall, 91.1% and 99.3% of the target and non-target particles are respectively collected at their respective outlets. These

results demonstrate that the integrated device indeed is highly efficient in capturing and isolating target particles by magnetic manipulation.

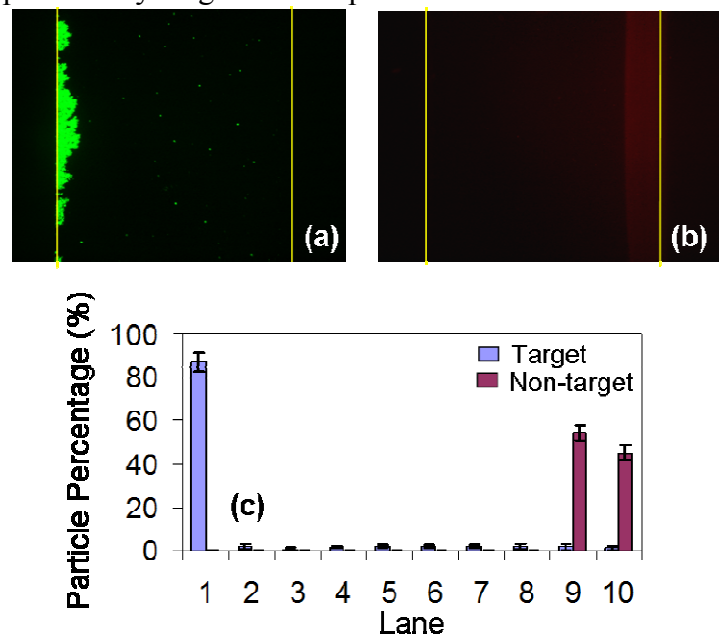

Figure 6. Distribution of target and non-target particle across the channel width at the exit of the separator with 1:1 mixture ratio of the target vs. non-target particles. (a) Fluorescent image of the target particles. (b) Fluorescent image of the non-target particles. The yellow lines mark the channel contours. (c) Distribution of the target and non-target particles in transverse lanes across the channel width.

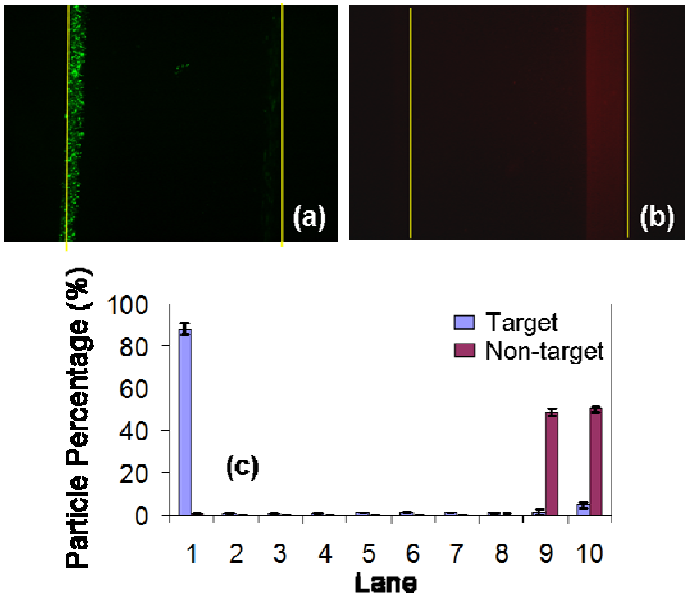

Figure 7. Distributions of target and non-target particles across channel width at the exit of the separator with 1:10 mixing ratio of the target vs. non-target particles. (a) Fluorescent image of the target particles. (b) Fluorescent image of the non-target particles. The yellow lines mark the channel

contours. (c) Distribution of target and non-target particles in transverse lanes across the channel width.

5. Conclusions

A novel integrated microchip for specific capture and separation of target microparticles using magnetic manipulation in continuous flow has been presented. The chip utilizes surface-functionalized magnetic beads as a vehicle of magnetic manipulation, which promotes mixing and capture of target particles by specific ligand-receptor binding, enhance mixing, and selectively separate target particle-bead complexes from non-target particles. Comprised of an incubator and a separator connected in series, the chip exploits the synergetic effects of laminar hydrodynamic flow and magnetic force to achieve target particle capture and fractionation. In contrast to existing particle separation devices, this approach offers simplicity in device fabrication and operation, and can potentially allow cell assays to be rapidly performed with high specificity and selectivity.

With judiciously selected geometrical parameters, the device was fabricated using soft lithography techniques. Experiments were conducted to systematically characterize the incubator and separator at the component level, as well as the integrated device. Experimental results have demonstrated the device is capable of specifically capturing, isolating and extracting target particles in a highly efficient, continuous manner.

First, the incubation module serves dual purposes of active mixing and capture of target particles. Active mixing can be attributed to the stream-crossing of magnetic beads by as well as flow agitation caused by the bead movement (relative to the flow stream). This facilitates the interaction between target particles and magnetic beads, thereby promoting the ligand-receptor binding based capture process.

Second, the separation module capitalizes on the magnetically actuated fractionation. Under the action of the magnetic field, magnetic beads are deflected laterally into a pure buffer stream and exit from the target exit. Experimental results have demonstrated that 90.3% of the magnetic beads are concentrated within the leftmost lane (Lane 1) in the separator channel. In addition, 96.2% of all magnetic beads are located within the left half of the channel and can be extracted from the target outlet.

Finally, the integrated chip incorporating both the incubator and separator has been tested using samples with two distinctly different ratios of target to non-target particles (1:1 and 1:10). In both cases, more than 90% of target particles in the sample are captured, isolated and extracted at the target outlet of the device. Meanwhile, more than 99% of non-target particles in the sample are retrieved at the device's waste outlet, confirming that the extract obtained at the target outlet is practically free of non-target particles. Thus, the device can be an effective tool for purification and enrichment of biological samples.

Acknowledgments

This research was supported in part by the National Science Foundation under award numbers CCR-0325344 and DBI-0650020.

References

1. Chabert M. and Viovy J.L., *Microfluidic high-throughput encapsulation and hydrodynamic self-sorting of single cells.* Proceedings of the National Academy of Sciences of the United States of America, 2008. **105**(9): p. 3191-3196.
2. Lien K.Y., Lee W.C., Lei H.Y., et al. *Integrated reverse transcription polymerase chain reaction systems for virus detection*. 2007 p. 1739-1748.
3. Murthy S.K., Sethu P., Vunjak-Novakovic G., et al., *Size-based microfluidic enrichment of neonatal rat cardiac cell populations.* Biomedical Microdevices, 2006. **8**(3): p. 231-237.
4. Zheng T., Yu H.M., Alexander C.M., et al., *Lectin-modified microchannels for mammalian cell capture and purification.* Biomedical Microdevices, 2007. **9**(4): p. 611-617.
5. Chen X., Cui D.F., Liu C.C., et al., *Continuous flow microfluidic device for cell separation, cell lysis and DNA purification.* Analytica Chimica Acta, 2007. **584**(2): p. 237-243.
6. Chmela E., Tijssen R., Blom M., et al., *A chip system for size separation of macromolecules and particles by hydrodynamic chromatography.* Analytical Chemistry, 2002. **74**(14): p. 3470-3475.
7. Huang L.R., Cox E.C., Austin R.H., et al., *Continuous particle separation through deterministic lateral displacement.* Science, 2004. **304**(5673): p. 987-990.
8. Jain A. and Posner J.D., *Particle dispersion and separation resolution of pinched flow fractionation.* Analytical Chemistry, 2008. **80**(5): p. 1641-1648.
9. Yamada M., Kano K., Tsuda Y., et al., *Microfluidic devices for size-dependent separation of liver cells.* Biomedical Microdevices, 2007. **9**(5): p. 637-645.
10. Petersson F., Nilsson A., Holm C., et al., *Continuous separation of lipid particles from erythrocytes by means of laminar flow and acoustic standing wave forces.* Lab on a Chip, 2005. **5**(1): p. 20-22.
11. Hu X.Y., Bessette P.H., Qian J.R., et al., *Marker-specific sorting of rare cells using dielectrophoresis.* Proceedings of the National Academy of Sciences of the United States of America, 2005. **102**(44): p. 15757-15761.
12. Huang Y., Joo S., Duhon M., et al., *Dielectrophoretic cell separation and gene expression profiling on microelectronic chip arrays.* Analytical Chemistry, 2002. **74**(14): p. 3362-3371.
13. Fu A.Y., Chou H.P., Spence C., et al., *An integrated microfabricated cell sorter.* Analytical Chemistry, 2002. **74**(11): p. 2451-2457.
14. Wang M.M., Tu E., Raymond D.E., et al., *Microfluidic sorting of mammalian cells by optical force switching.* Nature Biotechnology, 2005. **23**(1): p. 83-87.
15. Lien K.Y., Lin J.L., Liu C.Y., et al., *Purification and enrichment of virus samples utilizing magnetic beads on a microfluidic system.* Lab on a Chip, 2007. **7**(7): p. 868-875.
16. Pamme N. and Wilhelm C., *Continuous sorting of magnetic cells via on-chip free-flow magnetophoresis.* Lab on a Chip, 2006. **6**(8): p. 974-980.
17. Furdui V.I. and Harrison D.J., *Immunomagnetic T cell capture from blood for PCR analysis using microfluidic systems.* Lab on a Chip, 2004. **4**(6): p. 614-618.
18. Earhart C.M., Wilson R.J., White R.L., et al. *Microfabricated magnetic sifter for high-throughput and high-gradient magnetic separation*. 2009 p. 1436-1439.
19. Ahn C.H., Allen M.G., Trimmer W., et al., *A fully integrated micromachined magnetic particle separator.* Journal of Microelectromechanical Systems, 1996. **5**(3): p. 151-158.
20. Choi J.W., Oh K.W., Thomas J.H., et al., *An integrated microfluidic biochemical detection system for protein analysis with magnetic bead-based sampling capabilities.* Lab on a Chip, 2002. **2**(1): p. 27-30.
21. Deng T., Prentiss M., and Whitesides G.M., *Fabrication of magnetic microfiltration systems using soft lithography.* Applied Physics Letters, 2002. **80**(3): p. 461-463.
22. Recktenwald D. and Radbruch A., eds. *Cell separation methods and applications*. 1998, Marcel Dekker, Inc.: New York. 331.
23. Berger M., Castelino J., Huang R., et al., *Design of a microfabricated magnetic cell separator.* Electrophoresis, 2001. **22**(18): p. 3883-3892.
24. Inglis D.W., Riehn R., Austin R.H., et al., *Continuous microfluidic immunomagnetic cell separation.* Applied Physics Letters, 2004. **85**(21): p. 5093-5095.
25. Espy M.A., Sandin H., Carr C., et al., *An instrument for sorting of magnetic microparticles in a magnetic field gradient.* Cytometry Part A, 2006. **69A**(11): p. 1132-1142.
26. Chang C.C. and Yang R.J., *Electrokinetic mixing in microfluidic systems.* Microfluidics and Nanofluidics, 2007. **3**(5): p. 501-525.

27. Hessel V., Lowe H., and Schonfeld F., *Micromixers - a review on passive and active mixing principles.* Chemical Engineering Science, 2005. **60**(8-9): p. 2479-2501.
28. Nguyen N.T. and Wu Z.G., *Micromixers - a review.* Journal of Micromechanics and Microengineering, 2005. **15**(2): p. R1-R16.
29. Liu R.H., Stremler M.A., Sharp K.V., et al., *Passive mixing in a three-dimensional serpentine microchannel.* Journal of Microelectromechanical Systems, 2000. **9**(2): p. 190-197.
30. Stroock A.D., Dertinger S.K.W., Ajdari A., et al., *Chaotic mixer for microchannels.* Science, 2002. **295**(5555): p. 647-651.
31. Yang Z., Goto H., Matsumoto M., et al., *Active micromixer for microfluidic systems using lead-zirconate-titanate(PZT)-generated ultrasonic vibration.* Electrophoresis, 2000. **21**(1): p. 116-119.
32. El Moctar A.O., Aubry N., and Batton J., *Electro-hydrodynamic micro-fluidic mixer.* Lab on a Chip, 2003. **3**(4): p. 273-280.
33. Lin J.L., Lee K.H., and Lee G.B., *Active micro-mixers utilizing a gradient zeta potential induced by inclined buried shielding electrodes.* Journal of Micromechanics and Microengineering, 2006. **16**(4): p. 757-768.